Journal of Sound and Vibration 621 (2026) 119398

Contents lists available at ScienceDirect

Journal of Sound and Vibration

journal homepage: www.elsevier.com/locate/jsvi

Rapid Communications

Ray tracing via Snellius

Oskar Bschorr [a,1], Alessandro Bassetti [b,*]

[a] Independent Researcher
[b] Hamburg University of Technology, Structural Mechanics in Lightweight Design, Acoustics, Eissendorfer Str. 40, 21073, Hamburg, Germany

ARTICLE INFO

Keywords:
Snellius - law of refraction
Wave path
Geometrical acoustics
Wave path curvature
Curvature of the wavefront
Frenet frame coordinates

ABSTRACT

A wave travelling between two media denoted by different wave propagation velocities is subject to refraction at the interface between the media. The refraction is regulated by the Snellius law, where the interface is assumed infinitesimally thin. The jump in propagation velocity at the interface results in a discontinuous propagation direction for the wave. We consider a continuously changing medium, where the wave propagation velocity is assumed to be a continuous field. We reduce the Snellius law to its linear expansion at the interface between two regions of the medium with infinitesimally different propagation velocities. The linearised Snellius law connects the curvilinear coordinates associated with the propagation process from a point source and the spatial distribution of the propagation velocity. The coordinates map the rays evolving from the source and the wavefronts, orthogonal to the rays. Curved rays determine local osculating planes, spanned by the tangent to the ray and the gradient of the propagation velocity. The wavefront curvature is determined parallel to the tracing of each ray. Intersections of the wavefront are considered, with the osculating plane and with the longitudinal plane of the ray. For curved rays, the determined wavefront curvatures are different for the different planes. A numerical implementation of the model is used to approach an exemplary test case, regarding sound radiation in a stratified medium.

1. Introduction

The geometrical representation of wave propagation in an unbounded, continuous and inhomogeneous medium is the subject of the present work. We approach the problem by extending the Snellius law of refraction, which is valid for a discontinuity, to continuous refraction as it exists in the considered medium. In part we report the work by Bschorr [1], which is furthered by adding the kinematics of the wavefront in an infinitesimal ray tube. The linearised version of the Snell law is introduced in Section 2 and is used to relate variations of the propagation speed along a ray with the variation of the orientation of its tangent line. This enables the construction of a curvilinear coordinate system associated with the propagation from a point source or origin. The system of curvilinear coordinates is defined in Section 3. Its coordinates span the rays evolving from the origin and the wavefronts. The evolution of the wavefront is determined in terms of its curvature radius at the wave path. This result, whose derivation is presented in Section 5, was not known to the authors for arbitrary incidence. A solution for the perpendicular-incidence evolution of the wavefront curvature is reported in Appendix, this solution was derived by Bschorr and has been the starting point and the inspiration for the arbitrary-incidence solution. The results of the present theory are used to numerically solve an exemplary problem of sound radiation in a stratified medium. Ray paths and wavefront curvatures are calculated at various initial radiation angles from

* Corresponding author.
E-mail address: alessandro.bassetti@tuhh.de (A. Bassetti).
[1] Deceased.

https://doi.org/10.1016/j.jsv.2025.119398
Received 21 November 2024; Received in revised form 30 July 2025; Accepted 11 August 2025
Available online 29 August 2025

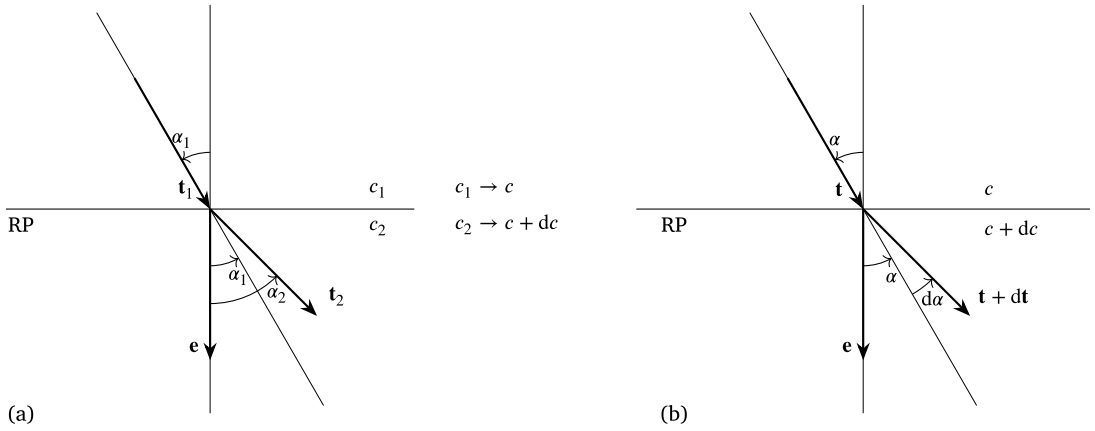

Fig. 1. Propagation between two media with the wave velocities c_1 and c_2, according to the refraction law (a). At the interface plane RP, the angle of incidence changes from α_1 to α_2 [rad]. In the case of infinitesimal refraction (b), a change in velocity from c to $c + \mathrm{d}c$ causes an angular deviation $\mathrm{d}\alpha$. RP Snellius refraction always takes place in the osculating plane (the drawing's plane), spanned by the direction vector $\mathbf{t}$ and the perpendicular vector $\mathbf{e}$.

a point source at zero altitude in the ICAO standard atmosphere. The numerical implementation and the corresponding results for the sound radiation are detailed in Section 7.

2. Snellius law

At the passage of a wave from a medium to a different one, the law of refraction states the following relation for the wave incidence to the interface between the media:

$$\frac{\sin \alpha_1}{c_1} = \frac{\sin \alpha_2}{c_2} \tag{1}$$

where c_1 and c_2 indicate the wave speeds [ms^{-1}] in the media. The schematic in Fig. 1(a) reports how the incidence of a wave is varied as it propagates through a planar interface RP between these media. According to Fig. 1(a), the angles α_1 and α_2 [rad] are the angles of the wave directions $\mathbf{t}_1$ and $\mathbf{t}_2$ [-] relative to the perpendicular direction $\mathbf{e}$ [-] of the refraction plane RP. The unit vector $\mathbf{e}$ is oriented towards the larger value of the wave speed, according to Eq. (1) and to the incidence α variation in Fig. 1(a). Note that angles between a reference vector and a second vector are positive, if an anticlockwise rotation sets the reference vector parallel to the second vector. In the case of infinitesimal refraction, at the local transition plane RP from a medium with the wave velocity $c_1 = c$ to one with $c_2 = c + \mathrm{d}c$, Fig. 1(b), the Snellius formula (1) can be stated as follows:

$$\frac{\sin \alpha}{c} = \frac{\sin (\alpha + \mathrm{d}\alpha)}{c + \mathrm{d}c} \tag{2}$$

The linearised Taylor expansion of Eq. (2) provides the infinitesimal angular change $\mathrm{d}\alpha$ caused by the infinitesimal change in wave velocity $\mathrm{d}c$:

$$\mathrm{d}\alpha = \frac{\sin \alpha}{\cos \alpha} \frac{\mathrm{d}c}{c} \tag{3}$$

The infinitesimal refraction corresponds to the propagation of a wave in a continuous inhomogeneous medium. In this medium, Eq. (3) can be used to determine the geometric course of a smooth curvilinear wave path. Locally, the refraction takes place in the osculating plane, or the drawing plane in Fig. 1(b), which is spanned by the unit vectors $\mathbf{t}$ and $\mathbf{e}$.

3. Propagation medium and ray coordinate system

The present analysis is based on an inhomogeneous, isotropic medium that is unlimited in all sides. The wave-propagation speed, characteristic of the medium, is a scalar field defined as a function of the global Cartesian coordinates (x, y, z) [m], such that $c = c\,(x, y, z)$. Parallel to the global Cartesian coordinates, it is convenient to introduce a ray coordinate system. This is a system of curvilinear coordinates (ξ, η, ζ) [m] that are associated with a wave propagation process within the medium, from a point source. A point $P = P(x, y, z)$ connected with a wave path, or ray, describes the curved trajectory of a point of the wavefront, at varying ξ. The evolution of the variable ξ denotes the evolution of the local wavefront, meaning that at constant ξ a wavefront at a given instant in time is spanned by varying η and ζ around zero, in proximity of the ray.

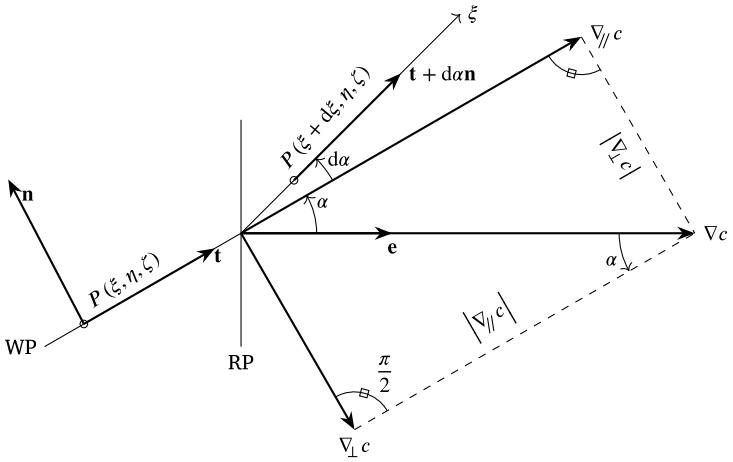

Fig. 2. Frenet frame at the path point P, for an infinitesimal refraction at the local refraction plane RP. The wave speed gradient ∇c lies orthogonally to the local refraction plane and is decomposed in its component along and orthogonally-to the path. The unit vectors **t** and **n** are both reported before the refraction and only **t** is reported after the refraction; the binormal **b** is orthogonal to the drawing plane and points the reader.

Connected to P and the ray, we use the Frenet coordinate system, with unit vectors **t**, **n** and **b**.

$$\begin{aligned} \mathbf{t} &= \frac{\mathrm{d}P}{\mathrm{d}\xi} \\ \mathbf{n} &= R\frac{\mathrm{d}\mathbf{t}}{\mathrm{d}\xi} \\ \mathbf{b} &= \mathbf{t} \times \mathbf{n} \end{aligned} \tag{4}$$

The tangent vector **t** [-] is associated with the running coordinate ξ [m]. It gives direction and orientation to the local wavefront velocity **c**. The normal **n** [-], with the running coordinate η [m], has the same direction and orientation as $\mathrm{d}\mathbf{t}/\mathrm{d}\xi$. It points in the direction of the centre of curvature of the wave path, at a distance R [m] from P. R is the radius of curvature of the path. The binormal **b** [-], with the running coordinate ζ [m], forms a right hand orthogonal basis with **t** and **n**; it runs then in the direction perpendicular to the osculating plane of the wave path in P. The tangent vector **t** and the normal vector **n** span the osculating plane. The tangent vector **t** and the binormal vector **b** span the longitudinal plane. The osculating plane has been introduced in Section 2, as being spanned by the local refraction-plane normal **e** and **t**. With the present definition of the wave speed field $c(x, y, z)$, the vector field given by the wave-speed gradient ∇c [s^{-1}] can be introduced. By noting that ∇c must lay perpendicular to any surface on which no variation of c is given, we can conclude that it is aligned at any point in space with the unit vector $\mathbf{e} = \mathbf{e}(x, y, z)$, perpendicular to the local refraction plane. This can be expressed as follows:

$$\nabla c = |\nabla c|\,\mathbf{e} \tag{5}$$

The gradient vector ∇c can be composed as sum of two vectors $\nabla_{/\!/} c$ and $\nabla_\perp c$, corresponding to the given curvilinear coordinates, see Fig. 2.

$$\nabla c = \nabla_{/\!/} c + \nabla_\perp c \tag{6}$$

$$\nabla_{/\!/} c = \nabla c \cdot \mathbf{t}\,\mathbf{t} \tag{7}$$

$$\nabla_\perp c = \nabla c \cdot \mathbf{n}\,\mathbf{n} \tag{8}$$

In Section 4, we show that the term $\nabla_\perp c$ is related to the curvature κ [m^{-1}] of the wave path. As visible in Fig. 2, $\nabla_\perp c$ has a negative component along **n**. The component $\nabla_{/\!/} c$ determines the variation in curvature of the wavefront, due to variations of c along the wave path, as discussed in Sections 5 and 6.

4. The wave path and its radius of curvature

A wave propagating in the direction **t** is subject to a change $\mathrm{d}c$ in its propagation speed, when moving in an inhomogeneous medium by an infinitesimal step $\mathrm{d}\xi$ along its path:

$$\mathrm{d}c = \nabla c \cdot \mathbf{t}\mathrm{d}\xi \tag{9}$$

According to Eq. (3), a change in velocity $\mathrm{d}c$ causes a change in angle $\mathrm{d}\alpha$. Eqs. (3) and (9) provide a relationship between the infinitesimal step along the wave path $\mathrm{d}\xi$ and the associated change in direction $\mathrm{d}\alpha$:

$$\mathrm{d}\alpha = \frac{|\nabla c|}{c}\sin\alpha\ \mathrm{d}\xi \tag{10}$$

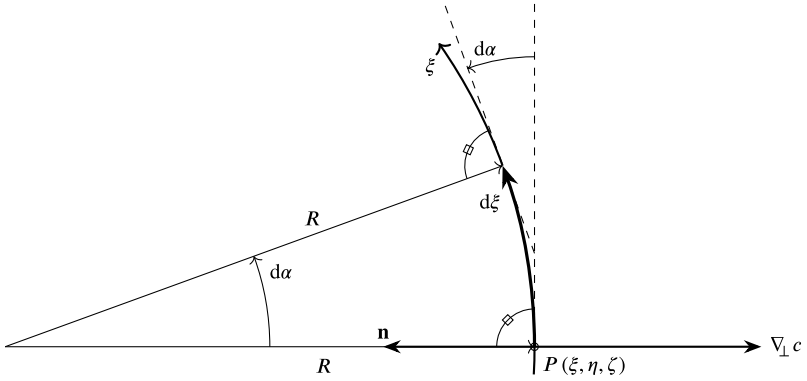

Fig. 3. Propagation on the local refraction plane and radius of curvature R [m] of the path, for a wave propagation in an inhomogeneous medium. A curved wave path that has a change in direction $\mathrm{d}\alpha$ for a path amplitude $\mathrm{d}\xi$, has a radius of curvature $R = \mathrm{d}\xi/\mathrm{d}\alpha$.

The connection between the wave path increment $\mathrm{d}\xi$ and the angular variation $\mathrm{d}\alpha$ is given by the path's curvature radius R, where $\mathrm{d}\xi = R\mathrm{d}\alpha$, see Fig. 3. The amplitude of the signed curvature κ of the wave path follows as:

$$|\kappa| = \frac{1}{R} = \frac{|\nabla c|}{c}\,|\sin\alpha| = \frac{|\nabla_\perp c|}{c} \tag{11}$$

The sign of κ, coincides with the sign of the path rotation induced by the step along the path, see Eq. (10). It is positive for reference observers in the half space pointed by **b**. The solution (11) for the curvature of the wave path is equivalent to the solution identified in Section "3-8" of Ref. [2]: "The radius of curvature of the ray path is $c/|\nabla_\perp c|$, or $c/(|\nabla c|\sin\theta_0)$, where θ_0 is the angle between the ray direction and the direction of ∇c." As explained in Section 3, the propagation speed gradient has a negative component along the normal direction **n**. This implies that the wave path bends in the plane of ∇c and **t**, in direction opposite to $\nabla_\perp c$. The normal vector of the Frenet frame is given as follows:

$$\mathbf{n} = \frac{c}{|\nabla_\perp c|}\frac{\partial \mathbf{t}}{\partial \xi} = -\frac{\nabla_\perp c}{|\nabla_\perp c|} \tag{12}$$

5. The wavefront and its curvature radius in the osculating plane

For a spherical wave in a homogeneous medium, the propagation between a source and a receiver follows a rectilinear path and the radius of curvature r of the wavefront is identical to the source—receiver distance. In an inhomogeneous medium, the propagation between a source and an observer is bent by variations of c, exception given by wave paths parallel to ∇c. The identity between source—observer distance and r is lost and 2 designations are necessary: measured from the source point at $\xi = 0$, a path point $P = P(\xi)$ has the path distance ξ [m] and additionally the wavefront radius of curvature $r = r(P)$ [m]. The radius of curvature is then a function of the spatial coordinates and of the speed of sound field c such that:

$$r = r\left(c\left(\xi,\eta,\zeta\right),\xi,\eta,\zeta\right) \tag{13}$$

The variation of r along a wave path, where η and ζ are zero, can be expressed as follows:

$$\mathrm{d}r = \left(\frac{\partial r}{\partial \xi} + \frac{\partial r}{\partial c}\frac{\partial c}{\partial \xi}\right)\mathrm{d}\xi = \left(1 + \frac{\partial r}{\partial c}\nabla c\cdot\mathbf{t}\right)\mathrm{d}\xi \tag{14}$$

where we used the identity between ξ and r at constant c to set $\partial r/\partial\xi = 1$. In order to determine the evolution of r from a source, we need to evaluate its variation at varying propagation speed. In order to do that we can again use the concept of local refraction and apply the Snellius law (1). In Fig. 4 we report a schematic of the refraction for an infinitesimal ray tube around a path, which has an incidence α to the interface plane, orthogonal to ∇c. The ray tube includes the wavefront segment $\mathrm{d}\eta$ at the interface. The boundaries of the ray tube intersect at a virtual source S which is the centre of the osculating circle of the wavefront included in the tube, or the local origin of r. The angles β and γ indicate the incidence of the tube boundaries before refraction. These boundaries are ray paths themselves, meaning that crossing the interface plane induces a change of incidence regulated by the Snellius law. After refraction, these incidence angles are denoted with β' and γ', and the Snellius law states

$$(c + \mathrm{d}c)\sin\beta = c\sin\beta', \qquad (c + \mathrm{d}c)\sin\gamma = c\sin\gamma' \tag{15}$$

We now express the aperture of the ray tube in terms of the wavefront segment included in the tube and its local curvature radius to the virtual source S.

$$\gamma - \beta = \frac{\mathrm{d}\eta}{r}, \qquad \gamma' - \beta' = \frac{\mathrm{d}\eta'}{r'} \tag{16}$$

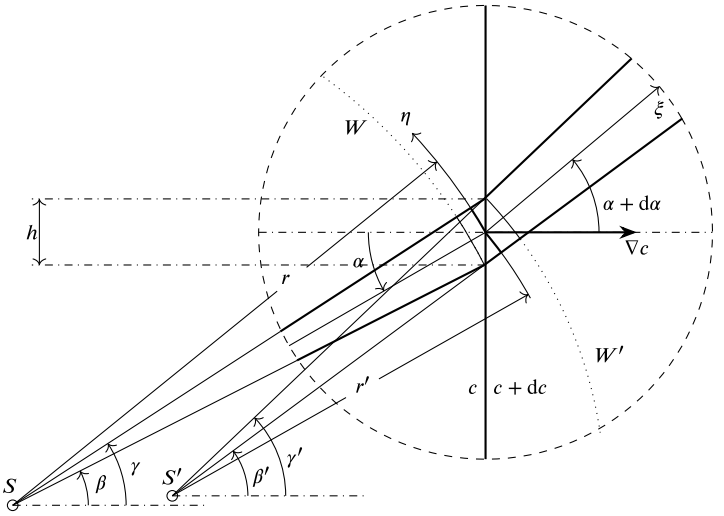

Fig. 4. Variation of the radius of curvature r [m] of the wavefront in a local refraction process implying a variation $\mathrm{d}c$ of the wave speed. An infinitesimal ray tube around a given path is represented with wavefronts W and W' before and after refraction. The wavefronts are given with respect to a virtual source position S, which is at the centre of the local osculating circle of the wavefront. The refraction displaces S to S' through two effects: a rotation and a change in curvature of the wavefront. The change in curvature is given by the variation of the radius of curvature from r to r' and represents the refraction-induced variation of the local spreading, from $\gamma - \beta$ to $\gamma' - \beta'$, corrected by the contraction of η, from $\mathrm{d}\eta$ to $\mathrm{d}\eta'$.

As reported in Fig. 4, the position of the virtual source S is changed through the refraction to S' by two effects: the rotation of the path and the variation of r. The rotation of the path causes a variation of the length of the wavefront included in the ray tube, which can be conveniently expressed as

$$\mathrm{d}\eta = h\cos\beta, \qquad \mathrm{d}\eta' = h\cos\beta' \tag{17}$$

where h is the segment of the interface plane included in the ray-tube, which is invariant to the refraction. Eq. (17) is only valid for an infinitesimal ray tube, where $\beta \to \alpha$ and $\gamma \to \alpha$. For the sake of the following demonstration, it is written in terms of β. By expressing γ' in terms of its refraction induced variation, $\gamma' = \gamma + \mathrm{d}\gamma$, we proceed to expand the Snellius law (15) in Taylor series around γ, which to first order in $\mathrm{d}\gamma$ is given as follows:

$$\frac{\mathrm{d}c}{c}\sin\gamma = cos\gamma\mathrm{d}\gamma \tag{18}$$

The harmonic functions of γ contained in (18) can be expressed in terms of β by using (16). The first order terms of their expansions around β are given as

$$\sin\gamma = \sin\beta + \frac{\mathrm{d}\eta}{r}\cos\beta, \qquad \cos\gamma = \cos\beta - \frac{\mathrm{d}\eta}{r}\sin\beta \tag{19}$$

The angle γ is defined as follows by using Eqs. (16) and (17):

$$\gamma = \beta + \frac{h}{r}\cos\beta \tag{20}$$

The variation of γ as a consequence of the refraction can be expressed as differential of (20)

$$\mathrm{d}\gamma = \mathrm{d}\beta - \frac{h}{r}\sin\beta\mathrm{d}\beta - \frac{h}{r^2}\cos\beta\mathrm{d}r \tag{21}$$

which can be written again in terms of $\mathrm{d}\eta$, to yield

$$\mathrm{d}\gamma = \left(1 - \frac{\mathrm{d}\eta\sin\beta}{r\cos\beta}\right)\mathrm{d}\beta - \frac{\mathrm{d}\eta}{r^2}\mathrm{d}r \tag{22}$$

By introducing Eq. (22) and expressions (19) in the linearised Snellius formula (18), we obtain

$$\frac{\mathrm{d}c}{c}\left(\sin\beta + \frac{\mathrm{d}\eta}{r}\cos\beta\right) = \left(\cos\beta - \frac{\mathrm{d}\eta}{r}\sin\beta\right)\left(\left(1 - \frac{\mathrm{d}\eta\sin\beta}{r\cos\beta}\right)\mathrm{d}\beta - \frac{\mathrm{d}\eta}{r^2}\mathrm{d}r\right) \tag{23}$$

After manipulation and simplification through the linearised Snellius rule, written for β analogously to Eq. (18), Eq. (23) can be stated as follows:

$$\frac{\mathrm{d}c}{c}\left(1 + 2\left(\frac{\sin\beta}{\cos\beta}\right)^2\right) = -\frac{\mathrm{d}r}{r} + \mathrm{o}(\mathrm{d}\eta) \tag{24}$$

In the limit $d\eta \to 0$, $\beta \to \alpha$, Eq. (24) is

$$\frac{dc}{c}\,\frac{1+(\sin\alpha)^2}{(\cos\alpha)^2} = -\frac{dr}{r} \tag{25}$$

Eq. (25) states the first order variation of the wavefront curvature radius r due to a propagation-speed variation dc. The expression can be used to determine the partial derivative of r at varying c:

$$\frac{\partial r}{\partial c} = -\,\frac{1+(\sin\alpha)^2}{(\cos\alpha)^2}\,\frac{r}{c} \tag{26}$$

By introducing the latter into Eq. (14) one gets the total derivative of r as:

$$\frac{dr}{d\xi} = 1 - \frac{1+(\sin\alpha)^2}{(\cos\alpha)^2}\,\frac{r}{c}\nabla c\cdot\mathbf{t} \tag{27}$$

By developing the scalar product, Eq. (27) can be written as follows:

$$\frac{dr}{d\xi} = 1 - r\frac{1+(\sin\alpha)^2}{\cos\alpha}\,\frac{|\nabla c|}{c} \tag{28}$$

The evolution of r along a wave path can be obtained by integrating Eq. (28):

$$r = \int_0^{\xi}\left(1 - r\frac{1+(\sin\alpha)^2}{\cos\alpha}\,\frac{|\nabla c|}{c}\right)d\xi \tag{29}$$

The growth trend of r along the ray path and as a function of c is stated in Eq. (28), where the incidence $\alpha\epsilon(-\pi,\pi]$ sets the trend through the sign of the function $\cos(\alpha)$. This sign is in effect the sign of the scalar product between ∇c and $\mathbf{t}$, compare with Eq. (27). The radius r grows as a function of c when moving along the ray adversely to the gradient ∇c. By using the decomposition of ∇c introduced in Section 3, a decrease of r is observed if $\mathbf{t}$ is aligned with $\nabla_{/\!/} c$. On the contrary, r increases when $\mathbf{t}$ and $\nabla_{/\!/} c$ are oriented opposite to each other. The deviation of r from the geometrical distance to the source is then the product of the amplitude of $(r/c)\nabla c$ with the incidence factor $B(\alpha)\cos\alpha$, where the positive factor $B(\alpha)$ is defined as

$$B(\alpha) = \frac{1+(\sin\alpha)^2}{(\cos\alpha)^2} \tag{30}$$

The $B(\alpha)$ factor is, from an analytical point of view, the new part of the present theory. It is an element which is of greatest relevance for radiation angles at large incidence, due to its singularity for $|\alpha| \to \pi/2$. Note that this singularity is not in contrast with the present theory, since propagation along the interface between media at (infinitesimally) different wave-propagation speeds ultimately breaks the wavefront and violates the phase-speed conservation on which the refraction law is based. The $B(\alpha)$ factor is also the non-intuitive part of the extrapolation of a perpendicular-incidence evaluation of r. The evaluation of r at nearly perpendicular incidence was made by the first author and it has been motivation and inspiration for the derivation in the present section. It is reported in Appendix. For $\alpha \to 0$ or $\alpha \to \pi$, the general-incidence solution in Eq. (29) coincides with the solution for nearly perpendicular incidence, compare with Eq. (A.6).

6. The wavefront curvature radius in the longitudinal plane

The variation of ray tube spreading through a variation of the wave velocity c is also observed in the local longitudinal plane, spanned by $\mathbf{t}$ and $\mathbf{b}$. While in the refraction plane the section of the wavefront is given by an arc $d\eta$, in the longitudinal plane we have an arc in $d\zeta$. Parallel to Section 5, we introduce a virtual source S_ζ at the centre of the osculating circle and the radius of curvature r_ζ of the wavefront. Since the situation in the longitudinal plane corresponds to a refraction at perpendicular incidence, Eq. (27) can be specialised for $\alpha = 0$, or equivalently for $\alpha = \pi$, to give the following differential equation for r_ζ.

$$\frac{dr_\zeta}{d\xi} = 1 - r_\zeta\frac{\nabla c\cdot\mathbf{t}}{c} \tag{31}$$

The evolution of r_ζ along the wave path is then given by the integral equation

$$r_\zeta = \int_0^{\xi}\left(1 - r_\zeta\frac{\nabla c\cdot\mathbf{t}}{c}\right)d\xi \tag{32}$$

The evolution of r_ζ varies through the factor (30) from the evolution of r.

7. Wave propagation discretisation and numerical calculation of sound propagation in a stratified medium

In order to substantiate the present theory we propose here an application example, based on the numerical calculation of ray paths and wavefront curvatures on a general medium with varying wave-propagation speed. The numerical approach to determine the wave path uses the first order approximation of the Snellius law, as described in Section 7.1. The evolution of the wavefront curvatures is made by numerically integrating the equations developed in the present theory, see Section 7.2. The application is on sound propagation through a stratified ideal atmosphere, where the present theory is applied to the standard-atmosphere model proposed by the International Civil Aviation Organization, see Section 7.3.

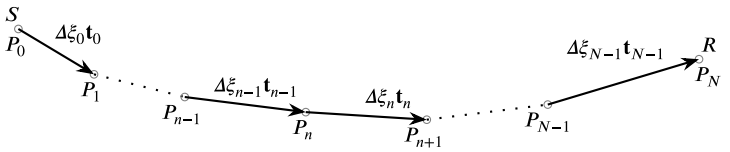

Fig. 5. Calculation of a wave path in an inhomogeneous medium from the start location S, in P_0 with radiation direction $\mathbf{t}_0$, to the receiver R, in P_N. The overall path is made up of a sequence of N steps of length $\Delta\xi_n$, where n = 0 to N-1 is the index of the transmitter—receiver evaluation points.

7.1. Determination of the wave path

The wave path between a starting point S and a receiving point R is determined by assuming an initial radiation direction $\mathbf{t}_0$ and by evolving from the location of S through the knowledge of the local wave-propagation speed c and its gradient ∇c. As sketched in Fig. 5, the course of the wave is approximated by the sequence of finite-length steps, where the nth step $\Delta\xi_n\mathbf{t}_n$ connects the evaluation point P_n to the next point in the sequence P_{n+1}. The local quantities evaluated at a point P_n are all indicated with the index n, such as its Cartesian coordinates (x_n, y_n, z_n), corresponding to the position vector $\mathbf{x}_n$ from the origin of the given coordinate system. Likewise, the propagation speed and its gradient are indicated by c_n and $(\nabla c)_n$. At the point P_n the vectors $\mathbf{t}_n$ and $(\nabla c)_n$ define a local incidence angle α_n. If $\mathbf{t}_n$ and $(\nabla c)_n$ are not parallel to each other, they define a local osculating plane for the path where a rotation of $\mathbf{t}_n$ about an angle $\Delta\alpha$ defines the orientation of $\mathbf{t}_{n+1}$. For the numerical calculation, the infinitesimals $\mathrm{d}\alpha$ and $\mathrm{d}\xi$ in Eq. (10) are expanded linearly to $\mathrm{d}\alpha \to \Delta\alpha$ and $\mathrm{d}\xi \to \Delta\xi$ to obtain the rotation $\Delta\alpha$ at any evaluation point as follows.

$$\Delta\alpha = \frac{|\nabla c|}{c} \sin\alpha \; \Delta\xi \tag{33}$$

By assuming a constant time step $\Delta\tau$, the step length is defined by the local propagation speed and the path evolution from a point P_n, pointed by the vector $\mathbf{x}_n$, is given by

$$\mathbf{x}_{n+1} = \mathbf{x}_n + c_n \Delta\tau \; \mathbf{t}_n \tag{34}$$

The beam direction $\mathbf{t}_{n+1}$ at P_{n+1} is rotated by the refraction angle $\Delta\alpha_n$ compared to $\mathbf{t}_n$.

$$\Delta\alpha_n = |\nabla c|_n \sin\left(\alpha_n\right) \; \Delta\tau \tag{35}$$

The rotation takes place in the refraction plane, spanned by the vectors $(\nabla c)_n$ and $\mathbf{t}_n$, with the axis of rotation $\mathbf{b}_n$

$$\mathbf{b}_n = \frac{(\nabla c)_n \times \mathbf{t}_n}{\left|(\nabla c)_n \times \mathbf{t}_n\right|} \tag{36}$$

A rotation of $\mathbf{t}_n$ by the angle $\Delta\alpha_n$ around the axis $\mathbf{b}_n$ states the propagation direction for the step $(n+1)$:

$$\mathbf{t}_{n+1} = \mathbf{t}_n \cos\left(\Delta\alpha_n\right) + \mathbf{n}_n \sin\left(\Delta\alpha_n\right) \tag{37}$$

where $\mathbf{n}_n$ is the normal unit vector of the accompanying tripod associated with the wave path in P_n. The radius of curvature of the path can be determined by using Eq. (11), whose evaluation at P_n gives

$$R_n = \frac{c_n}{\left|(\nabla c)_n \sin\left(\alpha_n\right)\right|} \tag{38}$$

7.2. Determination of the curvatures of the wavefront

For the wavefront intersection with the local refraction plane, the change $\mathrm{d}r$ of the curvature radius r with an infinitesimal wave-propagation speed change dc/c is expanded linearly according to (25) $\mathrm{d}c \to \Delta c$ and $\mathrm{d}r \to \Delta r$

$$\frac{\Delta r}{r} = -\frac{\Delta c}{c} \frac{1 + (\sin\alpha)^2}{(\cos\alpha)^2} \tag{39}$$

By applying Eq. (7), the variation of wave-propagation speed at the step n can be expressed as

$$\Delta c_n = \mathbf{t}_n \cdot (\nabla c)_n \, \Delta\xi_n = \mathbf{t}_n \cdot \mathbf{e}_n \, |\nabla c|_n \, \Delta\tau c_n = \cos\left(\alpha_n\right) |\nabla c|_n \, \Delta\tau c_n \tag{40}$$

The change of the radius of curvature of the wavefront intersection with the osculating plane, as induced by the variation of the propagation speed, is obtained as

$$\frac{\Delta r_n}{r_n} = -\frac{1 + \left(\sin\alpha_n\right)^2}{\cos\alpha_n} \; |\nabla c|_n \; \Delta\tau \tag{41}$$

The sequence for the evaluation of the curvature radius combines the direct increment, due to the step in wave-propagation direction, and Eq. (41) to yield the following:

$$r_{n+1} = r_n + \left(c_n - r_n \left|\nabla c\right|_n \frac{1 + \left(\sin \alpha_n\right)^2}{\cos \alpha_n} \right) \Delta\tau \tag{42}$$

where r at the step $n+1$ results from evaluations at the previous step n.

For the curvature radius of the wavefront intersection with the longitudinal plane, spanned by $\mathbf{t}$ and $\mathbf{b}$, we can specify (39) to perpendicular incidence and use it analogously as for r, in order to determine the increment of r_ζ at the given step. The value of r_ζ at the step $n+1$ results from evaluations at step n as follows:

$$r_{\zeta\ n+1} = r_{\zeta\ n} + \left(c_n - r_{\zeta\ n} \left|\nabla c\right|_n \cos \alpha_n \right) \Delta\tau \tag{43}$$

7.3. Wave propagation in a stratified medium

We consider a stratified medium in which the speed of sound varies as a function of the Cartesian coordinate z and a point source S is placed in the origin of the coordinate system. The medium is assumed to be a perfect gas where pressure p, density ρ and absolute temperature T are connected through the equation of state

$$p = \rho\ R\ T \tag{44}$$

where R [$\mathrm{Jkg^{-1}K^{-1}}$] has a constant value. For this medium, where we assume a constant value for the ratio $\gamma = c_p/c_V$ between the specific heat capacities at constant pressure c_p and at constant volume c_V, both with dimensions [$\mathrm{Jkg^{-1}K^{-1}}$], the speed of sound can be assumed a function of the absolute temperature T only. With this assumption, the speed-of sound profile at varying z is directly inferred by the absolute temperature profile. Such profile, including a piecewise linear trend for the temperature, is reported in Fig. 6(a). There we use the data associated with the standard atmosphere published by the International Civil Aviation Organization (ICAO), see Table 1 in [3], by adding the simplification that the geopotential and the geometrical altitudes coincide. Fig. 6(a) also includes the speed of sound as function of the temperature, as deduced from the following equation:

$$c = \sqrt{\gamma R T} \tag{45}$$

where $\gamma = 1.4$ and $R = 287.05\ \mathrm{Jkg^{-1}K^{-1}}$ are the values for dry air as a perfect gas, see Ref. [3]. A sound source is placed in the present example at zero altitude in the ICAO atmosphere and it is assumed to radiate sound uniformly in the half space at positive altitudes. We follow the evolution of rays in an arbitrary polar plane, associated with the source, where the polar axis is the vertical line at the source position, oriented towards growing altitude. At constant altitude, the speed of sound gradient is a constant vector, which lies parallel to the polar axis. Its orientation and amplitude will depend on the altitude and the corresponding temperature-variation gradient, by following the relation

$$\nabla c = \frac{1}{2} \sqrt{\frac{\gamma R}{T}} \nabla T \tag{46}$$

which derives from Eq. (45). According to the present theory and to the proposed atmosphere model, sound radiating horizontally from the source at zero altitude is bent upwards by following the surface of a "radiation sphere" centred above the source, tangent to the horizontal plane and having a radius of 88.66 km. This radius can be evaluated by introducing the standard-atmosphere static-temperature data, see Table 1 in Ref. [3], in Eqs. (45) and (46) (the static temperature gradient at zero altitude can either be deduced from the tabulated data or can be directly input by using the value of $-0.0065\ \mathrm{K\ m^{-1}}$ indicated in Table D of the introduction part in Ref. [3]) and by introducing the corresponding values for c and ∇c in Eq. (11). According to the present model, no sound radiation will occur in the neighbourhood of the source, outside of the radiation sphere. This implies the existence of a local zone of silence, which is given by cutting out the radiation sphere from the half space at non negative altitude around the source. This zone of silence is denoted "Antisphere of silence" in the present work. Numerical evaluations of ray tracing in a polar plane of the source at zero altitude are reported in the diagrams of Fig. 6(b). These evaluations are made by using a time step $\Delta\tau = 0.25$s and by ending the propagation at an altitude of 60 km, where we assume that the medium is too rarefied for acoustic-wave propagation. The numerical evaluation of the ray with initial polar angle tending to $\vartheta_0 = \pi/2$ follows the boundary of the antisphere of silence in the troposphere. The evaluations reported in Fig. 6(b) are made for rays departing the source at radiation directions $\mathbf{t}$ that form polar angles ϑ_0 spanning the interval $\theta_0 \in [0, \pi/2)$ with a constant step of $\pi/12$ rad. We note that the curvature of the rays correctly corresponds to the direction of ∇c, with centre of curvature opposite to the component $\nabla_\perp c$.

The evolution of the curvature of the wavefronts is reported in Fig. 7. The result, stemming from Eqs. (42) and (43), shows both the raw dependence of the wavefront curvature on the amplitude of $r\nabla c/c$ at normal incidence in the layers, see the diagram at $\vartheta_0 = 0$, and the effect of the incidence factor $\mathrm{B}(\alpha)\cos\alpha$ for larger values of ϑ_0. The effect of the factor $\mathrm{B}(\alpha)$, see Eq. (30), which makes the difference between the evolution of the wavefront radius in the osculating plane r and the one in the longitudinal plane r_ζ, is progressively more visible as the radiation direction gets shallower in the atmosphere and the angle ϑ_0 approaches $\pi/2$.

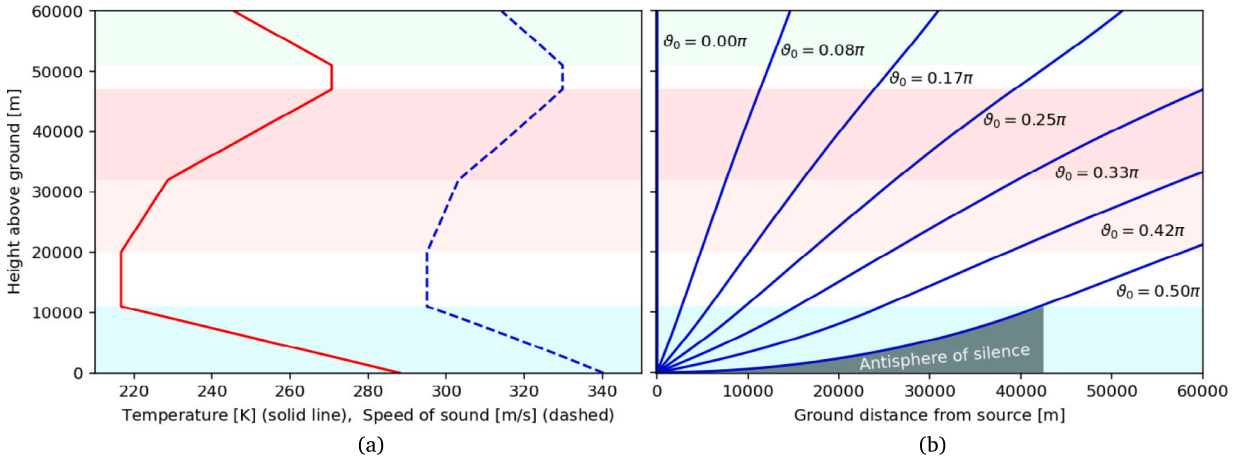

Fig. 6. (a) Temperature and speed of sound profiles at increasing altitude in the medium, according to the simplified ICAO standard atmosphere and by assuming the atmosphere made of ideal, dry air. (b) Ray tracing of a source at zero altitude in the standard atmosphere. The polar angle of the initial ray direction **t** is reported in the diagrams as ϑ_0, note that the polar axis is the vertical line at the source position, pointing positive altitudes. The zone of silence due to the zero-altitude speed-of sound gradient is reported as "Antisphere of silence", limited to the troposphere.

8. Conclusion

For wave refraction in inhomogeneous media with a continuous wave-velocity field, we generalised the Snellius law of refraction to the differential form given by Eq. (3) and we used it to describe the evolution of wavefronts in an inhomogeneous medium. The differential Snellius law, Eq. (3), connects rotations along the wave path to the variation of wave velocity in the medium. It is sufficient to determine a wave path and the local curvatures of the wavefront, provided the wave-velocity field and its gradient are known for the medium along the wave path. By using the Frenet accompanying frame along the wave path and Eq. (3) we determine its connection to the variable wave-speed field in the medium. The wave path has an osculating plane which is spanned by the gradient of the wave velocity ∇c and by the tangent vector to the path **t**. We decomposed ∇c into its components parallel and perpendicular to **t**:

> The perpendicular component $\nabla_\perp c$ is connected to the wave path geometry. The normal vector **n** of the Frenet frame is opposite to $\nabla_\perp c$ and the radius of curvature amounts to $c/|\nabla_\perp c|$, see Eqs. (11) and (12). This result is well known in ray acoustics, as reported in Section "8-3" of Acoustics by Pierce, Ref. [2].
>
> The parallel component $\nabla_{/\!/} c$ is associated with the geometry of the wavefront in the vicinity of the path. For the infinitesimal ray tube containing the wave path, we derived expressions for the variation of the wavefront curvature radii along the path, see Eqs. (29) for r and (32) for r_ζ. These expressions indicate that, at the presence of ray curvature, the wavefront has a curvature radius r in the osculating plane, which differs from the curvature radius r_ζ in the longitudinal plane.

The present result allows a full geometrical construction of the direct wave field emanating from a point in a free-space inhomogeneous medium, provided the wave velocity distribution in the medium is known and is a continuous field. The values of r and r_ζ of the wavefront are given in terms of integral equations, requiring a numerical procedure to determine their evolution from the source position. For a general medium we proposed a numerical solution for the Snellius ray tracing in the wave propagation from an arbitrarily placed point source. This general solution has been specified to the exemplary problem of a sound source at zero altitude, in the ICAO standard atmosphere. For this specific atmosphere and according to the present theory, direct sound radiation only occurs within a radiation sphere, which can be imagined standing on the ground at the source position, and being as tall as 20 times the highest mountain on Earth. The corresponding antisphere of silence is a volume in the vicinity of the source which is impenetrable to direct sound radiation. The numerical evaluation of the ray path from the source and initially directed parallel to the ground, closely follows the boundary of the antisphere of silence during its curvilinear propagation within the whole troposphere. The parallel evaluation of the wavefront curvature radii r and r_ζ, in the osculating and in the longitudinal planes, shows a large difference between the two parameters at shallow radiation angles. The difference is driven by the factor $\mathrm{B}(\alpha)$, see Eq. (30), which is equal to 1 at perpendicular incidence, grows with the incidence amplitude $|\alpha|$ and presents an asymptote for $|\alpha| \to \pi/2$. Sound radiation directed along the vertical to the ground occurs along a rectilinear path. In this case r and r_ζ coincide and deviate from the geometrical distance to the source, due to the sound-speed inhomogeneity. The deviation of r_ζ from the geometrical distance to the source is in general moderate, when compared to the deviations of r from the same distance. Rays that are mostly curved also have the largest wavefront curvature discrepancy between the osculating and the longitudinal planes.

CRediT authorship contribution statement

Oskar Bschorr: Writing – original draft, Methodology, Formal analysis, Conceptualization. **Alessandro Bassetti:** Writing – review & editing, Writing – original draft, Visualization, Formal analysis, Conceptualization.

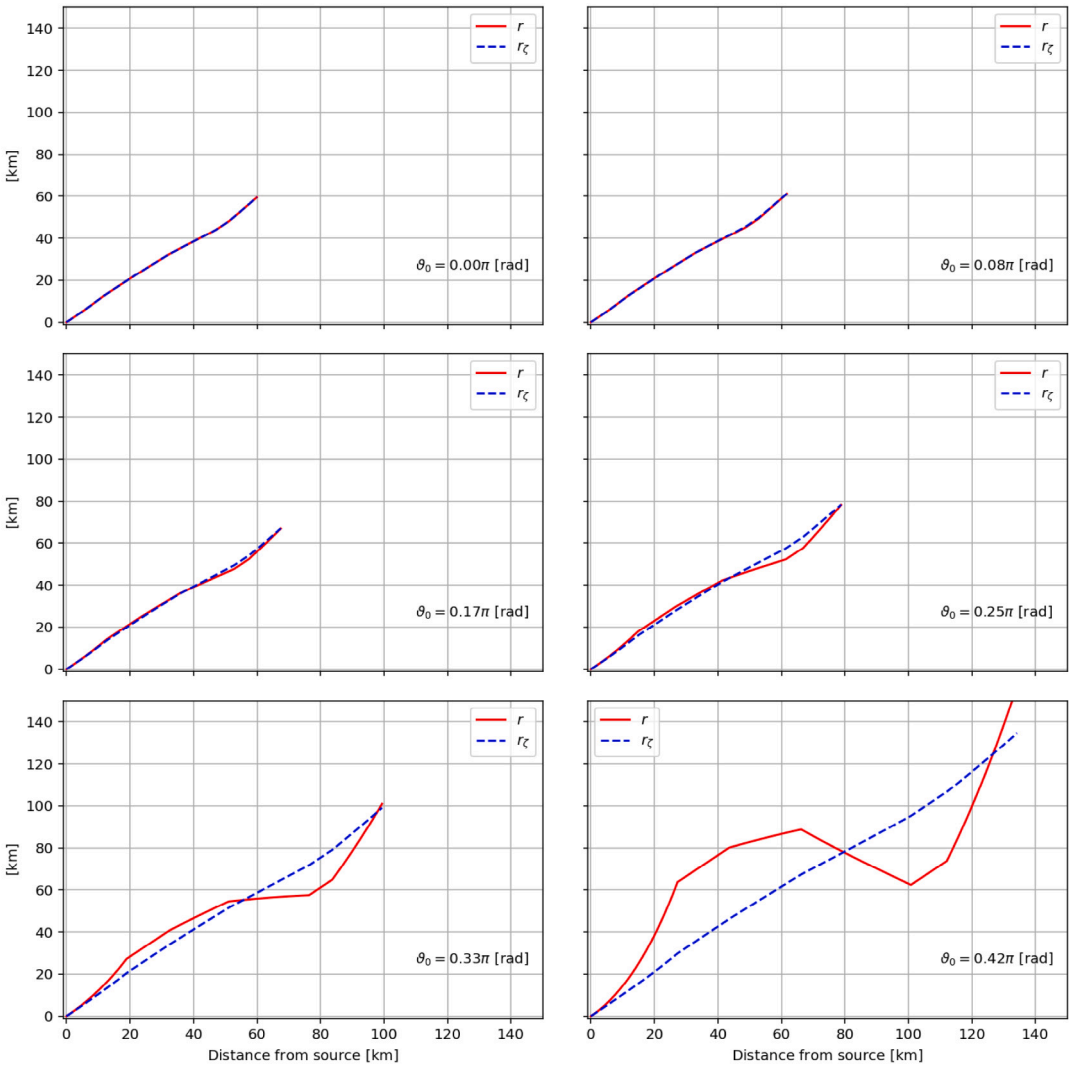

Fig. 7. Wavefront curvature radii r, in the osculating plane, and r_ζ, in the longitudinal plane, at varying initial polar angle ϑ_0 of the radiation direction. Note that in the present example the osculating plane coincides with the polar plane for the whole length of the wave path.

Declaration of competing interest

The authors declare that they have no known competing financial interests or personal relationships that could have appeared to influence the work reported in this paper.

Appendix. Wavefront curvature at perpendicular incidence

In source—receiver constellations corresponding to the limiting case $\alpha \to \{0, \pi\}$, with wave-propagation unit vector $\mathbf{t}$ and wave-velocity gradient direction $\mathbf{e}$ lying parallel to each other, we derive a solution for $r(\xi)$. The local incidence to the refraction plane is sketched in Fig. A.8 for the case $\mathbf{t} = -\mathbf{e}$, which implies a focusing effect of the propagation path or an increase of the wavefront curvature radius $r(\xi)$ resulting from the refraction effect.

If a wave with the wavefront curvature radius r and the infinitesimal angle of incidence $\mathrm{d}\alpha$ hits a refraction plane RP with the speed of sound variation $\mathrm{d}c$, this results in an angular deviation $\mathrm{dd}\alpha$. Because $\mathrm{d}\alpha$, $\mathrm{dd}\alpha \to 0$, the Snellius formula is simplified to:

$$\frac{\mathrm{d}\alpha}{c} = \frac{\mathrm{d}\alpha + \mathrm{dd}\alpha}{c + \mathrm{d}c} \tag{A.1}$$

By introducing (7), the above relation (A.1) reduces to

$$\frac{\mathrm{dd}\alpha}{\mathrm{d}\alpha} = \frac{\mathrm{d}c}{c} = \frac{\nabla c \cdot \mathbf{t}\,\mathrm{d}\xi}{c} \tag{A.2}$$

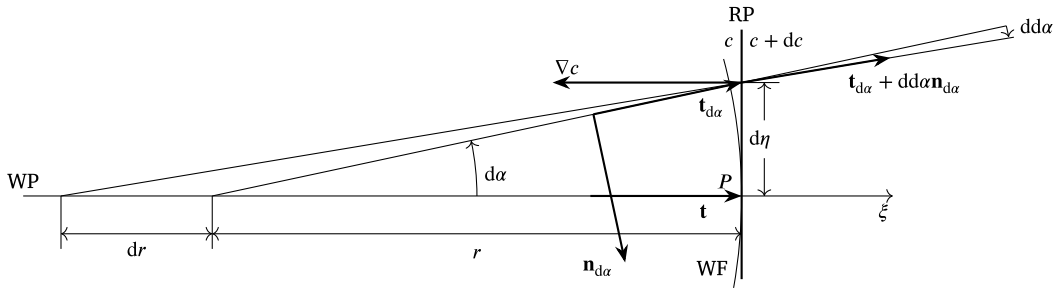

Fig. A.8. Special case $\alpha \to \pi$, with negative variation of the wave speed ($\mathrm{d}c < 0$) and $\mathbf{e} = -\mathbf{t}$. At the path point P, the wave travelling in the direction $\mathbf{t}$ has the wavefront WF with curvature radius r. In order to represent the angle change caused by an infinitesimal change in velocity $\mathrm{d}c$ at the refraction plane RP, we introduce an auxiliary beam with the infinitesimal angular deviation $\mathrm{d}\alpha$, or the distance $\mathrm{d}\eta$, from the path point P, and with a unit vector $\mathbf{t}_{\mathrm{d}\alpha}$ and a normal vector $\mathbf{n}_{\mathrm{d}\alpha}$, oriented according to $\mathbf{e}$. If the auxiliary beam hits the refraction plane RP, there is a change in angle $\mathrm{dd}\alpha$ and thus a change $\mathrm{d}r$ of the wavefront's curvature radius. For propagation direction opposite to $\mathbf{e}$, the speed of sound gradient reduces the beam spreading by inducing a larger r. The contrary happens with propagation in the direction of $\mathbf{e}$.

An angular difference $\mathrm{dd}\alpha$ changes the radius r by $\mathrm{d}r$. A small arc of the wavefront circle contained in the wave-path osculating plane is represented as $\mathrm{d}\eta$ in Fig. A.8. The logarithmic differentiation of the infinitesimal triangular relationship $\mathrm{d}\alpha = \mathrm{d}\eta/r$ yields the relationship with $\mathrm{d}\eta = \text{const}$.

$$\frac{\mathrm{dd}\alpha}{\mathrm{d}\alpha} = -\frac{\mathrm{d}r}{r} \tag{A.3}$$

Both Eqs. (A.2) and (A.3) combined give the change in radius $\mathrm{d}r$ caused by the transition of the wave from c to $c + \mathrm{d}c$, caused by the change in the coordinate along the wave path $\mathrm{d}\xi$.

$$\frac{\mathrm{d}r}{r} = -\frac{\mathrm{d}c}{c} = -\mathrm{sgn}\,(\mathbf{t}\cdot\mathbf{e})\,\frac{|\nabla c|}{c}\mathrm{d}\xi \tag{A.4}$$

In Eq. (A.4) we specialised Eq. (7) by using the identity $\mathrm{sgn}\,(\mathbf{t}\cdot\mathbf{e}) = (\mathbf{t}\cdot\mathbf{e})$, which is only valid in the limiting case $\alpha \to \{0, \pi\}$. In a homogeneous medium, if the wavefront advances by $\mathrm{d}\xi$ its curvature radius increases by $\mathrm{d}r = \mathrm{d}\xi$. This spreading must be combined with the effect of sound speed variation, in (A.4), to yield the net variation of the radius r for an infinitesimal step along the wave path:

$$\frac{\mathrm{d}r}{\mathrm{d}\xi} = 1 - \mathrm{sgn}\,(\mathbf{t}\cdot\mathbf{e})\,r\frac{|\nabla c|}{c} \tag{A.5}$$

The wavefront curvature radius can be obtained by integrating along the wave path:

$$r = \int_0^{\xi}\left(1 - \mathrm{sgn}\,(\mathbf{t}\cdot\mathbf{e})\,r\frac{|\nabla c|}{c}\right)\mathrm{d}\xi \tag{A.6}$$

As expected, in a uniform and homogeneous medium with $|\nabla c| = 0$ the source distance ξ and the wavefront curvature radius r are identical, according to (A.6).

Data availability

No data was used for the research described in the article.

References

[1] O. Bschorr, Bestimmung von Wellenpfaden via Snellius-Brechungsgesetz. OneWay-Wellengleichung, in: Fortschritte der Akustik - DAGA 2024, Deutsche Gesellschaft für Akustik e.V. (DEGA), Hannover, 2024, URL: https://pub.dega-akustik.de/DAGA_2024/files/upload/paper/5.pdf.
[2] A. Pierce, Acoustics – An Introduction to its physical principles and applications, Acoustical Society of America, 1991.
[3] International Civil Aviation Organization, ICAO, Manual of the ICAO Standard Atmosphere, extended to 80 kilometres, Technical Report, (Doc 7488/3) 1993.